VIBRATION SOURCE CHARACTERIZATION USING FORCE ANALYSIS TECHNIQUE AND A BAYESIAN REGULARIZATION

Charly Faure, Frédéric Ablitzer, Charles Pezerat, Jérôme Antoni

23rd International Congress on Sound & Vibration
Athens, Greece 10-14 July 2016
ICSV23

VIBRATION SOURCE CHARACTERIZATION USING FORCE ANALYSIS TECHNIQUE AND A BAYESIAN REGULARIZATION.

Charly Faure, Frédéric Ablitzer and Charles Pézerat
Laboratoire d'Acoustique de l'Université du Maine UMR CNRS 6613, Le Mans, France
email: charly.faure@univ-lemans.fr

Jérôme Antoni
Laboratoire Vibrations Acoustique, Univ Lyon, INSA-Lyon, LVA EA677, F-69621, Villeurbanne, France

The Force Analysis Technique (FAT) is a inverse method for the characterization of vibration sources applied on a structure, based on measurements of its displacement. From the knowledge of the local equation of motion of the structure, it allows both the localization and the quantification of sources, without the need of boundary conditions. As many inverse methods, the FAT is however highly sensitive to noise and includes traditionally a low pass filter to fix this instability. This work presents new strategies for the regularization step within the Bayesian framework. It introduces *a priori* probabilities which can lead to the Tikhonov regularization when Gaussian densities are used for both the source field and the noise, or to a sparse identification when using a Bernoulli-Gaussian *a priori* on sources. These two cases are performed by the Gibb's sampler, a particular Markov Chain Monte Carlo (MCMC) algorithm. It allows an unsupervised (or empirical) and automatic regularization besides confidence intervals on variables, especially on the source field.

1. Introduction

In vibration engineering, many efforts have been made to improve prediction methods apt to describe vibration propagation so as to provide better estimates of model outputs, such as displacement fields, yet the knowledge of the input sources still remains largely limited. In turn, this leads to unavoidable bias on the predicted outputs. Hence, the identification of vibration sources is an important topic of vibroacoustics. Different methods based on modal models or frequency response functions, including Transfer Path Analysis (TPA) described in Ref. [1] or Statistical Energy Analysis described (SEA) described in Ref. [2], have been developed. A review of some of these methods can be found in Ref. [3]. As these methods often need information about the structure, boundary conditions, position of sources or number of sources, they can be interpreted as global methods in opposite to local methods which only need local information about the structure. The Force Analysis Technique (FAT), used in this work and developed in Ref. [4], is precisely a local approach based on the numerical discretization of the equation of motion of the structure to identify the vibration force. Similarly to many inverse methods, the FAT is highly sensitive to measurement noise because it is interpreted as the result of several nonphysical sources instead of measurement perturbations. Traditionally, a supervised low pass filtering solves the instability issue. This work presents some improvements of the regularization procedure by the use of Bayesian approaches (see Ref. [5] and Ref. [6]). Various *a priori* information can be taken into account and formalized them mathematically within the Bayesian framework, making it more practical than the Tikhonov method (see Ref. [7]). To go further, Markov Chain Monte Carlo (MCMC) algorithms (see Ref. [8]) allow inference of the whole

a posteriori probability of unknown parameters from numerical sampling, yielding a better exploration of probabilities and confidence intervals. The Gibb's sampling (see Ref. [9]), a special case of MCMC algorithms used in this work, is particularly suited to problems where the probabilities have an analytical expression, such as the Gaussian or the gamma distributions. After this introduction, the FAT is presented in Section 2 followed by the presentation of Bayesian methods in Section 3. The conditional probabilities used for the Gibb's sampling are developed for a Gaussian and a sparse *a priori* on sources in Section 4 and Section 5, respectively. The experimental validation is presented in Section 6 before the conclusion in Section 7.

2. Source characterization

2.1 Equation of motion

The FAT is based on the equation of motion of a known structure. As an example, the method is presented on a beam within Euler-Bernoulli beam theory. The harmonic transverse displacement $w(x,\omega)$ of the beam satisfies Eq. (1),

$$E(1+j\eta)\frac{bh^3}{12}\frac{\partial^4 w(x,\omega)}{\partial x^4} - \rho bh\omega^2 w(x,\omega) = f(x,\omega), \tag{1}$$

where E is the Young's modulus, η is the loss factor, b is the width, h is the thickness, $w(x,\omega)$ is the harmonic transverse displacement at location x and at angular frequency ω, ρ is the density and $f(x,\omega)$ is the vibration source at location x and at angular frequency ω. The principle of the method is to evaluate the transverse displacement field by measurement and, knowing the rest of the terms of left hand side of Eq. (1), to calculate directly the vibration source applied on the structure.

2.2 Estimation of derivatives

The spatial derivative is estimated by numerical differentiation, using centered finite difference method at second order, from

$$\frac{\partial^4 w(x_i,\omega)}{\partial x^4} \approx \frac{1}{\Delta_x^4}\Big(w(x_{i+2},\omega) - 4w(x_{i+1},\omega) + 6w(x_i,\omega) - 4w(x_{i-1},\omega) + w(x_{i-2},\omega)\Big), \tag{2}$$

where Δ_x is the constant spatial sampling rate. Substituting Eq. (2) into Eq. (1) allows to identify the vibration source applied at location x_i without having to evaluate physical boundary conditions and displacement all over the domain, as proposed in Eq. (3)

$$E(1+j\eta)\frac{bh^3}{12}\frac{w(x_{i+2},\omega) - 4w(x_{i+1},\omega) + 6w(x_i,\omega) - 4w(x_{i-1},\omega) + w(x_{i-2},\omega)}{\Delta_x^4} - \rho bh\omega^2 w_i(x_i,\omega) = f(x_i,\omega). \tag{3}$$

Due to the spatial derivative, two displacement points are used at each boundary of the studied area, without allowing the evaluation of sources at these boundaries. At these points, the central stencil $[1;-4;6;-4;1]$ can then be substituted by the corresponding forward stencil $[3;-14;26;-24;11;-2]$ or the backward one $[-2;11;-24;26;-14;3]$ in order to increase the domain of source identification with the same number of measures. It is important to underline that Eq. (1) (and its discrete form in Eq. (3)) describes locally the dynamic comportment of an elementary part of the structure. Consequently, if displacements and derivatives of displacement are known in a subpart of the structure (by measurement), the calculation of the force distribution in this subpart is possible without other information outside the subpart. Physical boundary conditions of the structure and displacement field

outside the studied area can then be ignored. In practice, this "local" property of the inverse method presents a real advantage over global methods, which depend on boundary conditions (i.e. modal analysis) and/or need a description of displacement field on the whole domain of the structure.

2.3 Matrix formulation

In the following, the equation of motion given by Eq. (3) will be used in matrix form

$$\boldsymbol{D}\boldsymbol{w} = \boldsymbol{f}, \tag{4}$$

where $\boldsymbol{D}$ is a $N \times N$ symmetric matrix resulting of the discretization of the structural operator by forward, central and backward stencils, $\boldsymbol{w}$ is the $N \times 1$ vector of displacement and $\boldsymbol{f}$ is the $N \times 1$ vector of vibration sources. As each measurement includes noise, the equation of observation is given by

$$\boldsymbol{y} = \boldsymbol{w} + \boldsymbol{n}, \tag{5}$$

where $\boldsymbol{y}$ is the $N \times 1$ vector of observed displacement and $\boldsymbol{n}$ is the $N \times 1$ vector of noise. Applying the method of source identification to the accessible quantity $\boldsymbol{y}$ yields

$$\boldsymbol{D}\boldsymbol{y} = \boldsymbol{f} + \boldsymbol{D}\boldsymbol{n}. \tag{6}$$

$\boldsymbol{n}$ is often much lower than $\boldsymbol{w}$ but $\boldsymbol{D}$ is a differential operator. As the displacement field remains mainly smooth while the noise is completely random, the term $\boldsymbol{D}\boldsymbol{n}$, called aberrant forces, can quickly becomes much higher than $\boldsymbol{f}$, making difficult the source identification. Thus, a regularization step is needed.

3. Regularization within the Bayesian framework

In lots of methods, an especially in inverse methods, some quantities are uncertain and sometimes completely unknown. Working with a probabilistic point of view is then a suitable approach to take into account these uncertainties. The Bayesian framework used in this work allows to include the *a priori* information in the identification process.

3.1 Bayes' theorem

Bayes proposed the following theorem to infer the probability of an event from both experiences and *a priori* knowledge

$$[A \mid B] = \frac{[B \mid A]\,[A]}{[B]} \propto [B \mid A]\,[A]\,. \tag{7}$$

$[A \mid B]$ is the conditional probability of A knowing B, it is called the *a posteriori* probability density and refers to the solution of the inverse problem. $[B \mid A]$ is the likelihood which expresses the information extracted from the experience (the direct problem). $[A]$ stands for the probability density of the random variable A, it is called the *a priori*. $[B]$ is called the "evidence" and acts as a constant to ensure that the integral of $[A \mid B]$ is equal to 1. Only the shape of the *a posteriori* density is used to evaluate the most probable solution (i.e. the regularized solution). As it is not impacted by the evidence, the proportional relationship is preferred in Eq. (7) rather than the absolute equality.

3.2 Gibb's sampling

The Gibb's sampling, a particular case of Markov Chain Monte Carlo (MCMC) algorithms, is used for the inference of the whole joint probability of all the random variables of the problem. With $[\Theta]$ the joint probability of the random variables $\Theta = \{\theta_1, \theta_2, \ldots, \theta_L\}$, the Gibb's sampling consists in sampling consecutively, until the convergence is reached, in each conditional probability $[\theta_n \mid \infty_{-\theta_n}]$, with n from 1 to L (the notation $\infty_{-\theta_n}$ stands for all the variables except θ_n). Then, histograms can be computed for each variable to identify its most probable value and the associated confidence intervals.

3.3 Hierarchical model

These conditional probabilities needed for the Gibb's sampling are not always easy to obtain. Hierarchical model, a way to represent relationships between random and deterministic variables of the problem into a multi-level Bayesian graph, is a particularly useful tool to calculate them from the following generic expression (see Ref. [10])

$$\left[\theta_j \mid \infty_{-\theta_j}\right] \propto \left[\theta_j \mid \text{Parents of } \theta_j\right] \times \prod_{\theta_k \text{ children of } \theta_j} \left[\theta_k \mid \text{Parents of } \theta_k\right] \tag{8}$$

For a specific variable of the graph θ_j, also called a *node*, links to other upper level variables, or *parent* nodes, act as its priors while links to lower level variables, or *children* nodes, represent its likelihood. The other parents of children nodes are called *co-parent* nodes. As a result of the Bayes theorem, the probability of a variable θ_j conditionally to all the others will only depend on its parents, children and co-parents.

4. Gaussian prior on sources

4.1 Priors

Considering an additive white noise $\boldsymbol{n}$ and a Gaussian *a priori* on sources,

$$[\boldsymbol{n}] \sim \mathcal{N}_c\left(\boldsymbol{n}; \mathbf{0}, \tau_n^{-1} \cdot \mathbf{I}\right) \tag{9}$$
$$[\boldsymbol{f}] \sim \mathcal{N}_c\left(\boldsymbol{f}; \mathbf{0}, \tau_f^{-1} \cdot \mathbf{I}\right) \tag{10}$$

where $\sim$ stands for "distributed as", τ_n and τ_f for the precision (i.e. the inverse of the variance) of noise and sources respectively, $\mathbf{I}$ for the identity matrix and the N-dimensional multivariate circular complex Gaussian density on $\boldsymbol{x}$ (see Ref. [11]) with mean vector $\boldsymbol{\mu}$ and covariance matrix $\boldsymbol{\Sigma}$ is defined as

$$\mathcal{N}_c\left(\boldsymbol{x}; \boldsymbol{\mu}, \boldsymbol{\Sigma}\right) = \frac{1}{\pi^M \mid \boldsymbol{\Sigma} \mid} \exp\left(\left(\boldsymbol{x} - \boldsymbol{\mu}\right)^H \boldsymbol{\Sigma}^{-1} \left(\boldsymbol{x} - \boldsymbol{\mu}\right)\right). \tag{11}$$

These two precisions are also unknown and follow *a priori* a gamma distribution

$$[\tau_n] \sim \mathcal{G}\left(\tau_n; \alpha_n, \beta_n\right) \tag{12}$$
$$[\tau_f] \sim \mathcal{G}\left(\tau_f; \alpha_f, \beta_f\right) \tag{13}$$

where the gamma density on x with shape parameter α and rate parameter β is expressed as

$$\mathcal{G}\left(x; \alpha, \beta\right) = \frac{\beta^\alpha}{\Gamma(\alpha)} \cdot x^{\alpha-1} \cdot \exp\left(-\beta \cdot x\right) \tag{14}$$

4.2 Hierarchical graph

Figure 1 shows the hierarchical graph corresponding to information given by Eqs. (6), (9), (10), (12) and (13). Square boxes stand for deterministic quantities while circular boxes correspond to random variables whose posterior distributions are to be inferred. Arrows represent direct relationship between quantities and $\mathcal{N}$ and $\mathcal{G}$ stand for Gaussian and gamma distributions respectively.

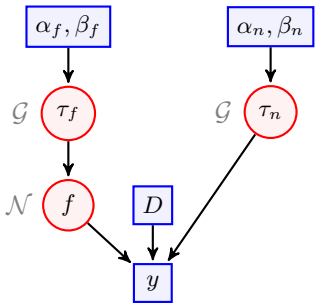

Figure 1: Hierarchical graph with a Gaussian *a priori* on sources.

4.3 Posteriors

Applying the Bayes theorem of Eq. (8) to the unknown quantities of interest $\boldsymbol{f}, \tau_n$ and τ_f yields

$$[\boldsymbol{f} \mid \infty_{-\boldsymbol{f}}] \propto \mathcal{N}_c\left(\boldsymbol{f}; \left(\boldsymbol{D}\boldsymbol{D}^H \tfrac{\tau_f}{\tau_n} + \mathbf{I}\right)^{-1} \boldsymbol{D}\boldsymbol{y}, \boldsymbol{D}\boldsymbol{D}^H \left(\boldsymbol{D}\boldsymbol{D}^H \tau_f + \tau_n \mathbf{I}\right)^{-1}\right) \tag{15}$$

$$[\tau_n \mid \infty_{-\tau_n}] \propto \mathcal{G}\left(\tau_n; \alpha_n + \tfrac{N}{2}, \left(\beta_n^{-1} + \tfrac{\|\boldsymbol{y} - \boldsymbol{D}^{-1}\boldsymbol{f}\|_2^2}{2}\right)^{-1}\right) \tag{16}$$

$$[\tau_f \mid \infty_{-\tau_f}] \propto \mathcal{G}\left(\tau_f; \alpha_f + \tfrac{N}{2}, \left(\beta_f^{-1} + \tfrac{\|\boldsymbol{f}\|_2^2}{2}\right)^{-1}\right) \tag{17}$$

where the superscript ^{H} stands for the Hermitian transformation.

5. Sparse prior on sources

5.1 Priors

Setting a Bernoulli-Gaussian *a priori* distribution on sources (see Ref. [12]) will act as a constraint leading to a sparser solution. The *a priori* probability of sources is then expressed as

$$[\boldsymbol{f}] = \prod_{i=1}^{N} [f_i] \sim \prod_{i=1}^{N} \mathcal{BG}(f_i; \lambda, \tau_f^{-1}) \tag{18}$$

where the Bernoulli-Gaussian density on x with sparsity parameter λ and precision τ_x is defined by

$$\mathcal{BG}(x; \lambda, \tau_x^{-1}) = (1-\lambda) \cdot \underbrace{\mathcal{N}_c(x; 0, 0)}_{\equiv \delta(x)} + \lambda \cdot \mathcal{N}_c(x; 0, \tau_x^{-1}) \tag{19}$$

The *a priori* probability of τ_f is the same as in Eq. (13) while λ is distributed *a priori* as

$$[\lambda] \sim \mathcal{B}e(\lambda; p, q) \tag{20}$$

where the Beta density on x with shape parameters p and q is given by

$$\mathcal{B}e(x; p, q) = \frac{\Gamma(p+q)}{\Gamma(p)\,\Gamma(q)} \cdot x^{p-1} \cdot (1-x)^{q-1} \tag{21}$$

5.2 Hierarchical graph

Changes of *a priori* in Section 5.1 yields a new hierarchical graph described in Fig. 2 with a fourth random variable to infer.

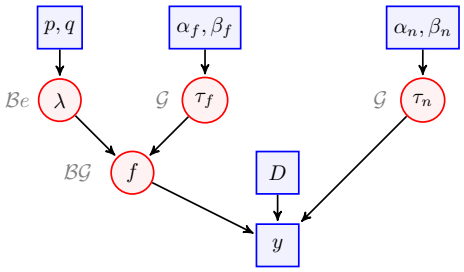

Figure 2: Hierarchical graph with a Bernoulli-Gaussian *a priori* on sources.

5.3 Posteriors

Applying the Bayes theorem of Eq. (8) to the unknown quantities of interest λ, $\boldsymbol{f}$, τ_n and τ_f yields new expressions, except for τ_n which is not impacted by the change of *a priori* on sources and so is the same as in Eq. (16). Introducing M the number of non-zero elements of $\boldsymbol{f}$,

$$[\lambda \mid \infty_{-\lambda}] \sim \mathcal{B}e(\lambda; p+N, q+M-N), \tag{22}$$

$$\left[\tau_f \mid \infty_{-\tau_f}\right] \sim \mathcal{G}\left(\tau_f; \alpha_f + \frac{M}{2}, \left(\beta_f^{-1} + \frac{\|\boldsymbol{f}\|_2^2}{2}\right)^{-1}\right). \tag{23}$$

Due to the difficulty to explore the probability space, the inference of $\boldsymbol{f}$ requires two conditions. First, multidimensional sampling of $\boldsymbol{f}$ should be replaced by a several unidimensional sampling of f_i. Secondly, each f_i should be distinguished into an amplitude r_i and a binary λ_i which can only take the value 1 to activate the source or 0 to force it to zero. The probability that each binary is equal to 1 is given by

$$[\lambda_i = 1 \mid \infty_{-\lambda_i}] = \left(1 + \frac{1-\lambda}{\lambda}\frac{\tau_n\|\boldsymbol{d}_i^{-1}\|_2^2 + \tau_f}{\tau_f}\mathrm{e}^{-\frac{\tau_n\|\boldsymbol{d}_i^{-H}\boldsymbol{e}_i\|_2^2}{\|\boldsymbol{d}_i^{-1}\|_2^2 + \frac{\tau_f}{\tau_n}}}\right)^{-1} \tag{24}$$

where $\boldsymbol{d}_i^{-1}$ is the i-th column of the inverse of matrix $\boldsymbol{D}$ and $\boldsymbol{e}_i = \boldsymbol{y} - (\boldsymbol{D}^{-1}\boldsymbol{f} - \boldsymbol{d}_i^{-1}f_i)$ the residue without the influence of f_i. If a sample drawn from the uniform distribution $\mathcal{U}([0;1])$ is greater than $[\lambda_i = 1 \mid \infty_{-\lambda_i}]$, the binary λ_i as well as the source f_i are set to 0. Otherwise, the corresponding amplitude is drawn from

$$[r_i \mid \infty_{-r_i}] \sim \mathcal{N}_c\left(r_i; \frac{\boldsymbol{d}_i^{-H}\boldsymbol{e}_i}{\|\boldsymbol{d}_i^{-1}\|_2^2 + \frac{\tau_f}{\tau_n}}, \left(\|\boldsymbol{d}_i^{-1}\|_2^2\tau_n + \tau_f\right)^{-1}\right) \tag{25}$$

6. Experimental validation

A freely suspended aluminum beam, whose dimensions are 72.25 cm $\times$ 2.96 cm $\times$ 2.9 mm, the Young modulus $E = 70 \times 10^9$ N/m^2, the mass density $\rho = 2700$ kg/m^3 and the structural damping $\eta = 10^{-4}$, is excited by a shaker located at $x_0 = 0.37$ m. A force sensor is placed at the interface to acquire a reference signal. The excitation signal is a linear chirp signal in frequency range $[100\,;4000]$ and the displacement measurement is performed by a scanning vibrometer with a mesh of 105 nodes and a constant spatial discretization $\Delta_x = 5.7$ mm. Pictures in Fig. 3 show the experimental setup. The Gibb's sampling is then performed at an arbitrary frequency of 1505 Hz for both *a priori* given in Section 4 and Section 5. To realize an empirical identification, *a priori* parameters are set so that p, q, α_n, α_f tend toward 0 and β_n, β_f tend toward $+\infty$, corresponding to non informative *a priori* information. Figure 4(a) shows the displacement measurements $\boldsymbol{y}$ while Fig.

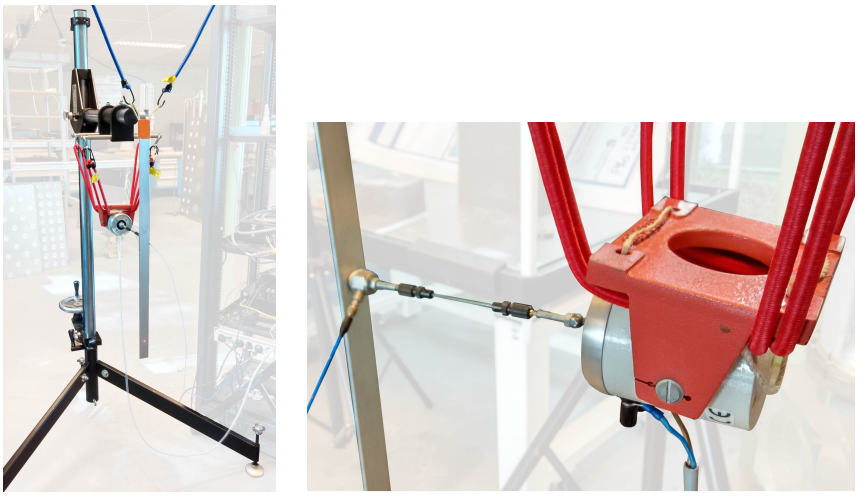

Figure 3: Experimental setup of the free beam excited by a shaker with a linear chirp signal in frequency range $[100; 4000]$ Hz. A force sensor is placed at the interface between the beam and the shaker to acquire a reference signal.

4(b) presents the corresponding source field recovered from the commonly used Tikhonov approach with Lcurve optimization (see Ref. [13]), from the MCMC procedure with Gaussian *a priori* with its 50% and 90% confidence intervals and from the MCMC procedure with sparse *a priori*. The MCMC solution with Gaussian *a priori* is quite close to the Lcurve one but it allows in addition the identification of confidence intervals and with only one scan of the structure. The BG solution shows a sparse solution with sources only between 0.3 and 0.4 cm. These fields are then spatially integrated to obtain the force in Newton injected into the structure and to compare with the reference signal. The Lcurve solution leads to an amplitude of -65.62 dB N (the reference value is 1 N), MCMC with Gaussian *a priori* yields an amplitude of -65.84 dB N, the sparse identification amplitude is -64.60 dB N while the reference amplitude given by the force sensor is -64.75 dB N.

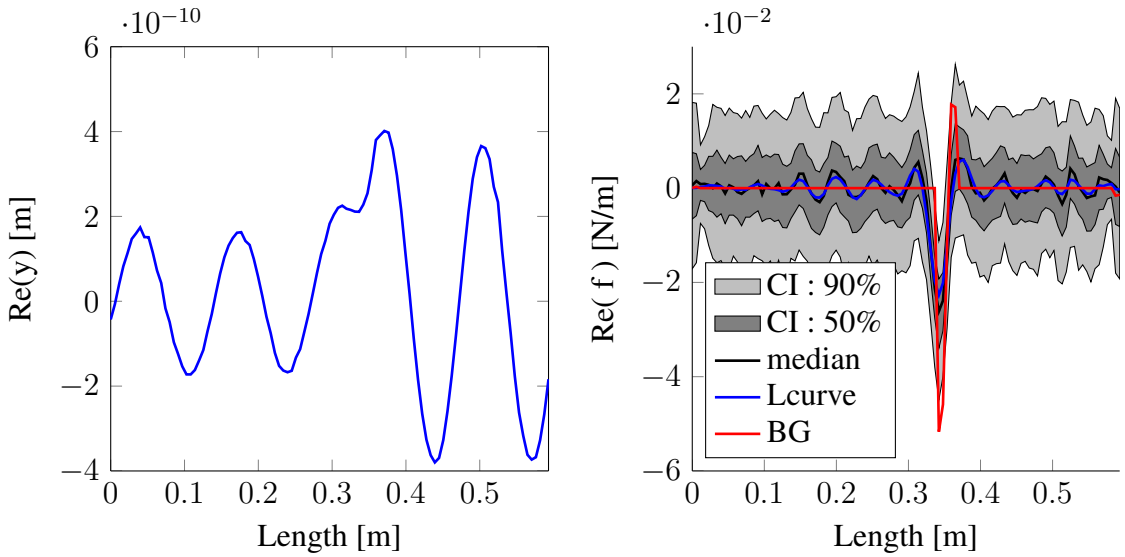

Figure 4: (a) Real part of the displacement field at 1505 Hz, (b) Real part of the associated regularized source distribution recovered from MCMC with Gaussian *a priori* with confidence intervals (gray shades), from MCMC with sparse *a priori* (BG) and from Lcurve.

7. Conclusion

This work presents new strategies for the regularization of the vibration source identification problem. The use of Bayesian methods, especially MCMC ones, allows an automatic and unsupervised regularization. With Gaussian *a priori* on sources, which is similar to the Tikhonov approach, the identification is time efficient and allows the evaluation of confidence intervals from a unique scan of the structure but shows residues outside the source location. With sparse *a priori*, the identification is forced to zero almost everywhere except at the source location. This last approach could be more efficient to detect and separate multiple sources. As an outlook, the Bayesian framework could also be used for the correction of the model of the structure.

REFERENCES

1. Janssens, K. H. B., Mas, P. P. G., Gajdatsy, P. A., Van Der Auweraer, H. and Gielen, L. J. P., (2014), *Transfer path analysis*. US Patent 8,731,868.
2. Lyon, R. H. and Lyon, R., *Statistical energy analysis of dynamical systems: theory and applications*, MIT press Cambridge (1975).
3. Dobson, B. and Rider, E. A review of the indirect calculation of excitation forces from measured structural response data, *Proceedings of the Institution of Mechanical Engineers, Part C: Journal of Mechanical Engineering Science*, **204** (2), 69–75, (1990).
4. Pezerat, C., *Méthode d'identification des efforts appliqués sur une structure vibrante, par résolution et régularisation du problème inverse*, Ph.D. thesis, INSA de Lyon, (1996).
5. Bolstad, W. M., *Introduction to Bayesian statistics*, John Wiley & Sons (2004).
6. Tarantola, A., *Inverse problem theory and methods for model parameter estimation*, siam (2005).
7. Tikhonov, A., *Solutions of ill-posed problems*.
8. Brooks, S., Gelman, A., Jones, G. and Meng, X.-L., *Handbook of Markov Chain Monte Carlo*, CRC press (2011).
9. Casella, G. and George, E. I. Explaining the gibbs sampler, *The American Statistician*, **46** (3), 167–174, (1992).
10. Bolstad, W. M., *Understanding computational Bayesian statistics*, vol. 644, John Wiley & Sons (2010).
11. Rice, J., *Mathematical statistics and data analysis*, Nelson Education (2006).
12. Bourguignon, S., Carfantan, H. and Idier, J. A sparsity-based method for the estimation of spectral lines from irregularly sampled data, *Selected Topics in Signal Processing, IEEE Journal of*, **1** (4), 575–585, (2007).
13. Hansen, P. C. Analysis of discrete ill-posed problems by means of the l-curve, *SIAM review*, **34** (4), 561–580, (1992).